

## New data on pyrochlore- and perovskite-group minerals from the Lovozero alkaline complex, Russia

ANTON R. CHAKHMOURADIAN<sup>1</sup>\*) and ROGER H. MITCHELL<sup>2</sup>)

<sup>1</sup>)Department of Geological Sciences, University of Manitoba, Winnipeg, Manitoba, Canada R3T 2N2

<sup>2</sup>)Department of Geology, Lakehead University, Thunder Bay, Ontario, Canada P7B 5E1

**Abstract:** Pyrochlore- and perovskite-group minerals are relatively common accessory constituents of agpaitic murmanite lujavrites at the Lovozero alkaline complex (Russia). These rocks contain euhedral crystals of niobian calcian loparite-(Ce) and, more commonly, ceroan lueshite that occurs as discrete oikocrysts and rims on the loparite-(Ce). The overall compositional range exhibited by these phases is  $(\text{Na}_{0.44-0.79} \text{REE}_{0.14-0.37} \text{Ca}_{0.02-0.12} \text{Sr}_{0.04-0.09} \text{Th}_{0-0.01}) (\text{Nb}_{0.12-0.66} \text{Ti}_{0.33-0.85} \text{Fe}_{0-0.01} \text{Ta}_{0-0.01}) \text{O}_3$ ; it agrees well with the evolutionary trend established previously for perovskite-group minerals from Lovozero. The murmanite lujavrites also contain early-crystallizing uranoan pyrochlore that subsequently underwent alteration to uranopyrochlore (5.0-26.4 wt.%  $\text{UO}_2$  for both) through interaction with a deuteritic fluid. The alteration pattern involves a decrease in Na, Ca and Sr contents from the core outward, increasing ionic deficiency in the *A* and *Y* sites, and progressive hydration. The proportion of relatively higher-charged cations does not change or slightly decreases toward the rim. The occurrence of lueshite and U-bearing pyrochlore in the murmanite lujavrites indicates that these rocks crystallized from the most evolved portion of a parental phonolitic magma. Pyrochlore-group minerals also occur in albite-rich, magnesio-arfvedsonite- and aegirine-bearing metasomatic rocks. These parageneses typically contain "silicified" varieties of pyrochlore exhibiting an oscillatory zoning pattern and, in some cases, superimposed secondary zoning. The metasomatic pyrochlore ranges from nearly stoichiometric Na-Ca-rich compositions to cation-deficient strontio-pyrochlore (up to 10.3 wt.% SrO) and plumbopyrochlore (up to 37.9 wt.% PbO). The oscillatory zoning involves variations in cation occupancy of the *A* site (primarily Na, Ca and Sr), and Si content. Elevated levels of Si (up to 16.8 wt.%  $\text{SiO}_2$ ) are invariably associated with the zones having the highest cation deficiency and  $\text{H}_2\text{O}$  contents. A negative correlation observed between the Si and (Nb+Ti) contents is interpreted to result from changes in pH,  $a(\text{SiO}_2)$ ,  $a(\text{Na}^{1+})$ ,  $a(\text{Ca}^{2+})$ , and activities of minor components during the crystal growth. Primary pyrochlore-group minerals from both lujavrites and albitites are characteristically poor in Ta (< 2.6 wt.%  $\text{Ta}_2\text{O}_5$ ), and enriched in Sr and light rare-earth elements. Comparative data on pyrochlore-group minerals from other alkaline-rock occurrences are presented.

**Key-words:** pyrochlore, lueshite, nepheline syenite, albitite, agpaitic rocks, Lovozero complex, Kola Peninsula, Russia.

### Introduction

The Lovozero alkaline complex in the Kola Alkaline Province (approximately 67°47' N, 34°45' E) is one of the most interesting of the family of sodic nepheline-syenite intrusions owing to its colossal size and remarkable degree of differentiation. The complex consists of several intrusive series emplaced in the Archean metamorphic rocks during the Devonian. The major series include: (1) porphyritic alkali and nepheline syenites; (2) poikilitic feldspathoid syenites; (3) a differentiated series consisting of alternating urtite, foyaite and lujavrite units; (4) eudialyte lujavrites; (5) murmanite lujavrites; and (6) alkaline lamprophyre dikes (Bussen & Sakharov, 1972). The mode of occurrence and textural features of series (5) are significantly different from typical lujavrites, and more consistent with their classification as phonolites (authors' unpubl. study). However, to avoid confusion, we shall refer to these rocks as

murmanite lujavrites, because they are known as such to most researchers familiar with the geology of Lovozero. Late-stage metasomatic (albite, aegirine-albite and amphibole-albite) rocks are very common at the margins of the complex, where they develop at the expense of earlier-crystallized intrusive suites and metamorphic wall rocks. The mineralogy of the Lovozero complex is described by Vlasov *et al.* (1966) and Semenov (1972). However, these two studies, as well as the recently published monographs of Khomyakov (1995) and Pekov (2000) focus primarily on alkaline pegmatites and associated hydrothermal parageneses; these rocks, although mineralogically unique, are volumetrically minor and very scarce (particularly, their well-differentiated types). Very few studies on the mineralogy and petrology of the major intrusive series have been undertaken since the publication of Bussen & Sakharov's (1972) work, and our knowledge of these rocks is utterly inadequate. Wet-chemical analyses of major minerals from

\*e-mail address of the corresponding author: CHAKHMOU@ms.umanitoba.ca

series (1) through (4) can be found in Bussen & Sakharov (1972). Interpretation of some compositional trends exhibited by rock-forming minerals from series (2)-(4) was provided by Borutskii (1988), although only limited analytical data are available in this monograph. Korobeinikov & Laajoki (1994) determined the evolutionary trend of pyroxene-group minerals from the nosean syenites toward the eudialyte lujavrites, and Mitchell & Chakhmouradian (1996) established the compositional variation of loparite-(Ce) across the same rock sequence. The details of mineralogy of the porphyritic syenites, murmanite lujavrites and dike rocks remain largely *terra incognita*. The available information on feldspars, amphiboles and feldspathoid minerals from the Lovozero intrusive series is insufficient to determine evolutionary trends of these minerals in cognate units (e.g., urtite  $\Rightarrow$  foyaite  $\Rightarrow$  lujavrite), or successive rock series (e.g., eudialyte lujavrites  $\Rightarrow$  murmanite lujavrites). With the exception of pegmatites, there are virtually no data on accessory phases from the unique peralkaline rocks that comprise the *bulk* of the intrusion.

In the present work, we describe the occurrence and composition of several pyrochlore- and perovskite-group minerals from different rock types exposed in the northern part of the complex. We do not attempt to provide a definitive study of pyrochlore occurrence at Lovozero, as the exposed area of the intrusion is about 600 sq. km, and further finds of pyrochlore-group minerals should be expected here. However, our work significantly expands the available knowledge of the relative distribution of these minerals in different rock types, and their compositional variation. For comparison, we also studied several samples of pyrochlore (*sensu lato*) from other alkaline complexes, including Vishnevye Mts. (Urals, Russia), Khibina (Kola Peninsula, Russia), Dara-i-Pioz (Tajikistan), Mont Saint-Hilaire (Québec, Canada), and Bearpaw Mts. (Montana, USA). The present work also provides new data on the occurrence and evolutionary trends exhibited by perovskite-group minerals from Lovozero, serving as a valuable addition to the previous works on that subject (Ifantopulo & Osokin, 1979; Kogarko *et al.*, 1996; Mitchell & Chakhmouradian, 1996).

## Background information

*Pyrochlore-group minerals* have the general formula  $A_{2-x}B_2O_6(OH,F,O)_{1-y} \cdot zH_2O$ , where the *A* site is occupied by large cations (Na, Ca, Sr, Pb, U, REE, etc.) and the *B* site primarily by Nb, Ti and Ta (Hogarth, 1989). Deuteric and secondary alteration of pyrochlore typically results in leaching of large weakly bonded cations from its structure and hydration. The maximum amount of  $H_2O$  that can be accommodated in the structure is estimated as  $1 + 3/8x$  where  $x$  is a cation deficiency at the *A* site (Ericit *et al.*, 1994). Pyrochlore-group minerals are subdivided into three subgroups differing in the proportion of major *B*-site cations: pyrochlore [(Nb+Ta) > 2Ti; Nb > Ta], betafite [(Nb+Ta) < 2Ti], and microlite [(Nb+Ta) > 2Ti; Ta > Nb]. Within these subgroups, minerals are further classified depending on whether any of the *A*-site cations, other than

Na or Ca, exceeds 20 at.% of the total occupancy in the *A* site (Hogarth, 1989). Such subsolidus processes as ion exchange or selective leaching are capable of changing the “identity” of pyrochlore-group minerals. Because these processes typically do not affect the Nb:Ti:Ta ratio in the *B* site, they tend to produce evolutionary trends that do not cross the boundaries between individual subgroups. Reported examples include conversion of uranoan pyrochlore to uranopyrochlore through preferential removal of Na and Ca from the structure, and retention of more strongly bound U (Chakhmouradian & Sitnikova, 1999). The effects of primary and secondary alteration on the chemistry of pyrochlore of different provenance were discussed by Lumpkin & Ewing (1995); unfortunately, however, their study did not cover apgaitic rocks.

In the early studies of Lovozero minerals (Vlasov *et al.*, 1966), pyrochlore-group phases were tentatively identified in several rock types, and primarily in nepheline-syenitic pegmatites. Very few wet-chemical analyses of these minerals are available in the literature. Hydrated pyrochlore (“hydropyrochlore”) was described from fenitic rocks at Mt. Vavnbed (as pseudomorphs after loparite), and from a pegmatite at Mt. Kuivchorr (as discrete crystals) by Semenov *et al.* (1963). Voloshin *et al.* (1989) found strontio-pyrochlore (0.20-0.62 *apfu* Sr) in albitites at Mt. Vavnbed (type locality for this species). Pyrochlore is traditionally interpreted as a characteristic mineral of miaskitic (“plumasitic”) parageneses, where it is typically associated with zircon and ilmenite (e.g., Semenov *et al.*, 1963). However, uranopyrochlore was recently observed in peralkaline rocks from Lovozero, including murmanite lujavrite at Mt. Selsurt (Chakhmouradian & Sitnikova, 1999), and a pegmatite vein intersected by the Karnasurt mine (Zadov *et al.*, 1999). All above localities are situated in the northern part of the complex (relative to Seid Lake); its southern portion remains very poorly explored.

Most of *perovskite-group minerals* are low-symmetry derivatives from the “ideal” cubic structure. Their general formula may be written as  $ABO_3$ , where the *A* site is occupied by large cations (Ca, Na, REE, Sr, Th, etc.) and the *B* site by Nb, Ti, Fe and minor Ta (Mitchell, 1996). Most of these phases are nearly stoichiometric; *A*-site vacancies (up to 0.2 *apfu*) have been observed predominantly among the REE-, Na-, and Th-rich species (e.g., Mitchell & Chakhmouradian, 1999). There is some evidence that the appearance of cation vacancies is accompanied by partial replacement of oxygen atoms in the perovskite framework with hydroxyl groups (Krivovichev *et al.*, 2000). Perovskite-group minerals are ubiquitous at Lovozero, locally gaining the status of a major rock-forming mineral (melanocratic nepheline syenites of series 3). Compositionally, these minerals are essentially members of the complex solid solution between (in order of decreasing significance) loparite-(Ce) ( $Na_{1/2}REE_{1/2}TiO_3$ ), lueshite ( $NaNbO_3$ ), perovskite ( $CaTiO_3$ ), and tausonite ( $SrTiO_3$ ) (Mitchell & Chakhmouradian, 1996). *Bona fide* lueshite has been identified in deuterically altered rocks of series (3), and as reaction rims on loparite-(Ce) from eudialyte lujavrites (series 4) (Semenov, 1972; Mitchell & Chakhmouradian, 1996).

Table 1. Petrographic and mineralogical characteristics of the pyrochlore- and lueshite-bearing samples from Lovozero.

Provenance	Rock type	Textural features	Major minerals	Accessory minerals
LVE2 Mt. El'morajok (SW slope)	Eudialyte lujavrite (intrusive series 4)	Unequigranular, medium- to fine- grained, mesocratic	Mc-perthite, Ne, Mg-Arf, Ae, Eud, Tit	Barian Lam, Nat, pyrochlore, strontian fluorapatite, pyrrhotite
LVV1 Mt. Vavnbed	Murmanite lujavrite (intrusive series 5)	Pseudoporphyrific, fine-grained, melanocratic	<i>Mesostasis</i> : Ne, Ae, Ab, Eud, Arf, Mg-Arf <i>Oikocrysts</i> : Mur	Nat, Kf, uranian pyrochlore, uranpyrochlore
LV54 Mt. Alluaiv (NE slope)	Murmanite lujavrite (intrusive series 5)	Pseudoporphyrific, fine-grained, melanocratic	<i>Mesostasis</i> : Kf, Ae, Ne, Sod, Ab, Eud <i>Phenocrysts</i> : Ne, Sod, Af <i>Oikocrysts</i> : Mur, Mg-Arf, Lmp	Ba-Lam, thorite, loparite-(Ce), lueshite, uranian pyrochlore
LV53a Mt. Alluaiv (NE slope)	Murmanite lujavrite (intrusive series 5)	Pseudoporphyrific, fine-grained, melanocratic	<i>Mesostasis</i> : Kf, Ae, Ne, Sod, Eud, Ab, Mg-Arf <i>Phenocrysts</i> : Ne, Sod, Af <i>Oikocrysts</i> : Mur, Lam	Nordite-(Ce), analcime, uranian pyrochlore, uranpyrochlore
LV71 Mt. Selsurt (N slope)	Albitized murmanite lujavrite	Poikiloblastic, fine-grained, mesocratic	<i>Mesostasis</i> : Ab, Kf, Mg-Arf <i>Inherited phenocrysts</i> : Ae <i>Poikiloblasts</i> : Lrz	Tit, strontian apatite, pyrochlore, Lam, Ba-Lam
LV72 Mt. Selsurt (N slope)	Albitite	Poikiloblastic, fine-grained, mesocratic	<i>Mesostasis</i> : Ab, Ae, Mg-Arf <i>Poikiloblasts</i> : Lrz, Eud astrophyllite	Kf, Cat, Rbd pyrochlore, fluorite
LV79 Mt. Selsurt (NW slope)	Albitite	Poikiloblastic, fine-grained, leuco- to mesocratic	<i>Mesostasis</i> : Ab, Ae, Mg-Arf <i>Poikiloblasts</i> : Narsarsukite	Cat, cryptomelane, fluorcapthite, Rbd, strontiopyrochlore, plumbopyrochlore
LV18 Mt. Karnasurt (NW slope)	Murmanite lujavrite (intrusive series 5)	Pseudoporphyrific, fine-grained, melanocratic	<i>Mesostasis</i> : Kf, Ae, Sod, Eud, Ab <i>Phenocrysts</i> : Ne, Sod <i>Oikocrysts</i> : Mur, Mg-Arf, Arf, Lam	Lueshite, nordite-(Ce) thorosteenstrupine, Ba-Lmp
LVE1 El'morajok Valley	Murmanite lujavrite (intrusive series 5)	Pseudoporphyrific, fine-grained, melanocratic	<i>Mesostasis</i> : Kf, Ae, Nat Mg-Arf, zeolites <i>Oikocrysts</i> : Mur, Mg-Arf	Rbd, Lam, lueshite, strontian hollandite, belyankinite

Mineral symbols: Ab albite, Ae aegirine, Af alkali feldspar, Arf arfvedsonite, Ba-Lam barytolamprophyllite, Cat catapleite, Eud eudialyte, Kf potassium feldspar, Lam lamprophyllite, Lrz lorenzenite, Mc microcline, Mg-Arf magnesioarfvedsonite, Mur murmanite, Nat natrolite, Ne nepheline, Rbd rhabdophane-(Ce), Sod sodalite, Tit titanite.

## Material studied and analytical techniques

Material for the present study was collected during several field trips to Lovozero from 1992-1998. None of the samples collected contain macroscopically visible crystals of niobate minerals; consequently, all samples were initially examined using optical and scanning electron microscopy combined with back-scattered electron imaging. Minute (< 150 µm) crystals of pyrochlore-group minerals were found in eight out of approximately 30 samples studied (the samples examined in this work are

briefly characterized in Table 1). Most of these crystals are euhedral to subhedral, octahedral or cubo-octahedral in habit, and range from reddish and yellowish brown to nearly colorless in thin section. In some metasomatic rocks, the crystals have a tabular habit owing to flattening along one of the [111] axes. Varieties with elevated U contents typically show a radiation-damage halo a few tens of µm in thickness. We did not observe any correlation between the morphology, color and composition of pyrochlore from Lovozero, although the U-enriched crystals appear to be somewhat darker-colored than "normal" pyrochlore.

Table 2. Representative compositions of pyrochlore-group minerals from intrusive rocks.

Wt.%	<i>pyrochlore</i>		<i>uranoan pyrochlore</i>		<i>uranpyrochlore</i>		<i>uranoan pyrochlore</i>		<i>uranoan pyrochlore</i>		<i>uranpyrochlore</i>
	1	2	3	4	5	6	7	8	9	10	11
Na <sub>2</sub> O	6.90	4.08	5.24	5.03	1.01	0.56	6.31	5.99	6.07	5.64	0.37
CaO	14.79	13.96	5.47	4.65	2.69	3.70	10.26	10.18	5.56	5.45	2.24
MnO	0.01	0.10	n.d.	0.05	n.d.	n.d.	n.d.	n.d.	n.d.	0.11	0.93
SrO	3.67	3.55	3.00	3.65	1.91	1.35	3.51	2.89	7.16	6.10	1.69
La <sub>2</sub> O <sub>3</sub>	0.47	0.65	1.17	2.05	2.04	1.37	1.71	1.71	2.13	1.50	0.76
Ce <sub>2</sub> O <sub>3</sub>	0.98	1.08	2.89	3.58	3.52	2.84	2.65	2.65	2.91	2.18	2.20
Pr <sub>2</sub> O <sub>3</sub>	n.d.	n.d.	n.d.	n.d.	n.d.	n.d.	0.07	0.06	0.34	0.04	n.d.
Nd <sub>2</sub> O <sub>3</sub>	n.d.	n.d.	1.04	0.50	0.47	0.43	0.77	0.54	0.49	0.85	0.76
UO <sub>2</sub>	0.89	0.85	20.73	22.59	26.35	25.46	4.99	10.97	8.66	15.16	19.62
Nb <sub>2</sub> O <sub>5</sub>	59.67	61.66	45.88	44.82	46.00	46.02	58.57	54.18	57.60	54.31	51.79
Ta <sub>2</sub> O <sub>5</sub>	0.23	0.73	1.94	1.84	1.57	1.87	0.96	1.54	1.30	1.63	2.57
TiO <sub>2</sub>	9.43	10.00	9.01	9.17	9.45	9.84	6.46	8.17	4.31	5.62	7.60
SiO <sub>2</sub>	0.36	0.29	n.d.	n.d.	n.d.	n.d.	n.d.	n.d.	n.d.	n.d.	n.d.
Fe <sub>2</sub> O <sub>3</sub>	0.08	0.09	n.d.	0.04	0.07	0.28	0.18	0.09	0.07	0.27	0.53
Total	97.48	97.05	96.37	97.97	95.08	93.72	96.44	98.97	96.60	98.86	91.06
Structural formulae ( $\Sigma B$ -site cations = 2)											
Na	0.774	0.440	0.725	0.704	0.138	0.075	0.771	0.746	0.793	0.743	0.047
Ca	0.917	0.832	0.418	0.360	0.203	0.274	0.693	0.701	0.401	0.397	0.159
Mn	-	0.005	-	0.003	-	-	-	-	-	0.006	0.052
Sr	0.123	0.118	0.124	0.153	0.078	0.054	0.128	0.108	0.280	0.240	0.065
La	0.010	0.013	0.031	0.055	0.053	0.035	0.040	0.041	0.053	0.038	0.019
Ce	0.021	0.022	0.075	0.095	0.091	0.072	0.061	0.062	0.072	0.054	0.053
Pr	-	-	-	-	-	-	0.002	0.001	0.008	0.001	-
Nd	-	-	0.026	0.013	0.012	0.011	0.017	0.012	0.012	0.021	0.018
U	0.011	0.011	0.329	0.363	0.413	0.392	0.070	0.157	0.130	0.229	0.289
$\Sigma A$	1.856	1.441	1.728	1.746	0.988	0.913	1.782	1.828	1.749	1.729	0.702
Nb	1.562	1.551	1.479	1.464	1.465	1.438	1.669	1.574	1.754	1.669	1.549
Ta	0.004	0.011	0.038	0.036	0.030	0.035	0.016	0.027	0.024	0.030	0.046
Ti	0.410	0.418	0.483	0.498	0.501	0.512	0.306	0.395	0.218	0.287	0.379
Si	0.021	0.016	-	-	-	-	-	-	-	-	-
Fe	0.003	0.004	-	0.002	0.004	0.015	0.009	0.004	0.004	0.014	0.026
$\Sigma B$	2.000	2.000	2.000	2.000	2.000	2.000	2.000	2.000	2.000	2.000	2.000

1-2 LVE2; 3-4 core and 5-6 rim of zoned crystals, LVV1; 7-8 LV54; 9 discrete unzoned crystal, and 10-11 core and rim of a zoned crystal, LV53a. Total Fe expressed as Fe<sub>2</sub>O<sub>3</sub>; n.d = not detected.

Perovskite-group minerals were found in three samples, and are represented by lueshite and, in one of the samples, also loparite-(Ce). Crystals of the latter mineral are subhedral to euhedral, whereas lueshite occurs as oikocrysts or overgrowths on loparite-(Ce). Both minerals are reddish brown in thin section, and weakly to distinctly anisotropic.

All mineral compositions were determined by X-ray energy-dispersion spectrometry using a Hitachi 570 scanning-electron microscope equipped with a LINK ISIS analytical system incorporating a Super ATW Light Element Detector (133 eV FWHM MnK). EDS spectra were acquired for 150 seconds (live time) with an accelerating voltage of 20 kV and beam current of 0.84-0.86 nA. The spectra were processed with the LINK ISIS-SEMQUANT software package, with full ZAF corrections applied. The following well-characterized natural and synthetic stan-

dards were employed for the analysis: loparite (Na, Nb, La, Ce, Pr, Nd), perovskite (Ca, Fe, Ti), corundum (Al), orthoclase (K), benitoite (Ba), manganian fayalite (Mn), wollastonite (Si), synthetic SrTiO<sub>3</sub> (Sr), YF<sub>3</sub> (Y, F), metallic Pb, Ta, Th and U. Because the samples of pyrochlore- and perovskite-group minerals studied are strongly altered and exhibit significant intragranular variation in composition, we did not attempt to use X-ray diffraction methods for their examination. Variation in unit-cell parameters of fresh and thermally treated pyrochlore depending on its chemistry has been previously discussed by a number of authors, including Krivokoneva & Sidorenko (1971), Hogarth & Horne (1989), and Marochkina (1990). The crystal chemistry of perovskite-group phases has been the subject of many recent papers, including several crystal-structure refinements (*e.g.*, Chakhmouradian *et al.*, 1999; Mitchell *et al.*, 2000).

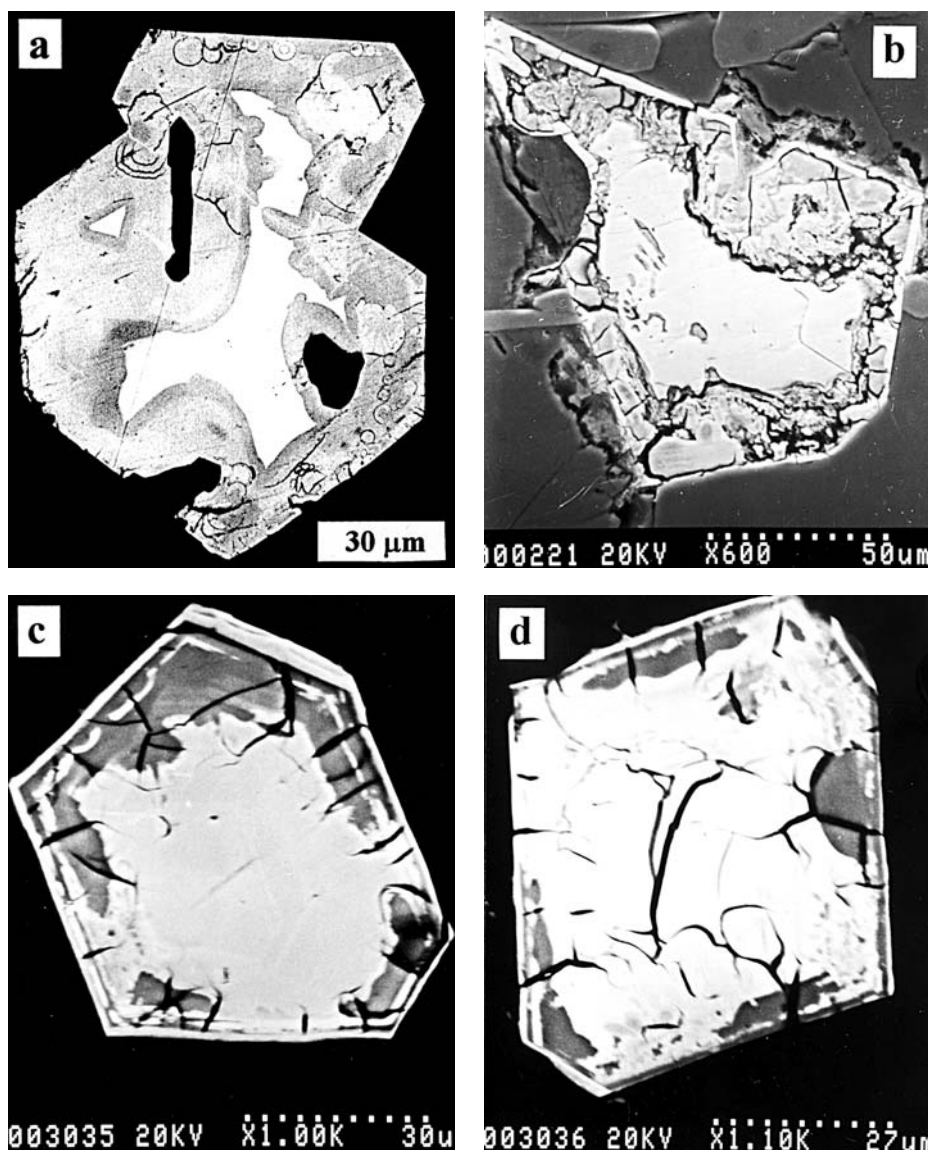


Fig. 1. Pyrochlore-group minerals from fresh (a-b) and albitized (c-d) murmanite lujavrites (BSE/SEM images). (a) Uranoan pyrochlore (white) altered to uranpyrochlore at the rim (gray), Mt. Vavnbed; (b) uranoan pyrochlore heavily fractured and altered at the rim, Mt. Alluaiv; (c) and (d) pyrochlore with secondary zoning superposed over weak primary (oscillatory) zoning, Mt. Selsurt.

## Occurrence and compositional variation

### Pyrochlore-group minerals

Pyrochlore from eudialyte lujavrite LVE2 is a relatively late-stage mineral confined to interstices, and associated with natrolite and titanite. Compositionally, it is nearly stoichiometric, and contains only minor *REE*, and moderate Sr plus Ti (Table 2, anal. 1-2). The crystals are devoid of detectable zoning.

In murmanite lujavrite LVV1, pyrochlore forms distinctly zoned crystals composed of *uranoan pyrochlore* in the core, and *uranpyrochlore* in the rim (Fig. 1a). The substitution mechanisms responsible for the incorporation of U in pyrochlore-group minerals have been discussed in detail in several previously published studies (*e.g.*,

Hogarth, 1989), and will not be considered here. The zoning pattern observed in LVV1 results from a decrease in Na, Ca and Sr contents from the core outward (Fig. 2 a-c). This change is accompanied by increase in the number of vacancies (Fig. 3a) and hydration of the mineral, as inferred from lower analysis totals (Table 2, anals. 3-6). In common with the uranoan pyrochlore-uranpyrochlore pair from Mt. Selsurt (Chakhmouradian & Sitnikova, 1999), the distribution of elements in the *B* site remains virtually unchanged (Fig. 2d, 3b). The primary uranoan pyrochlore is preserved only as irregular, commonly fragmented cores. The core is invariably surrounded by a “hydration front”, a thin intermediate zone with the lowest average atomic number (AZ). The accurate analysis of this material is impossible because of extensive beam damage at the spectrum-acquisition time chosen. The rim composed of uran-

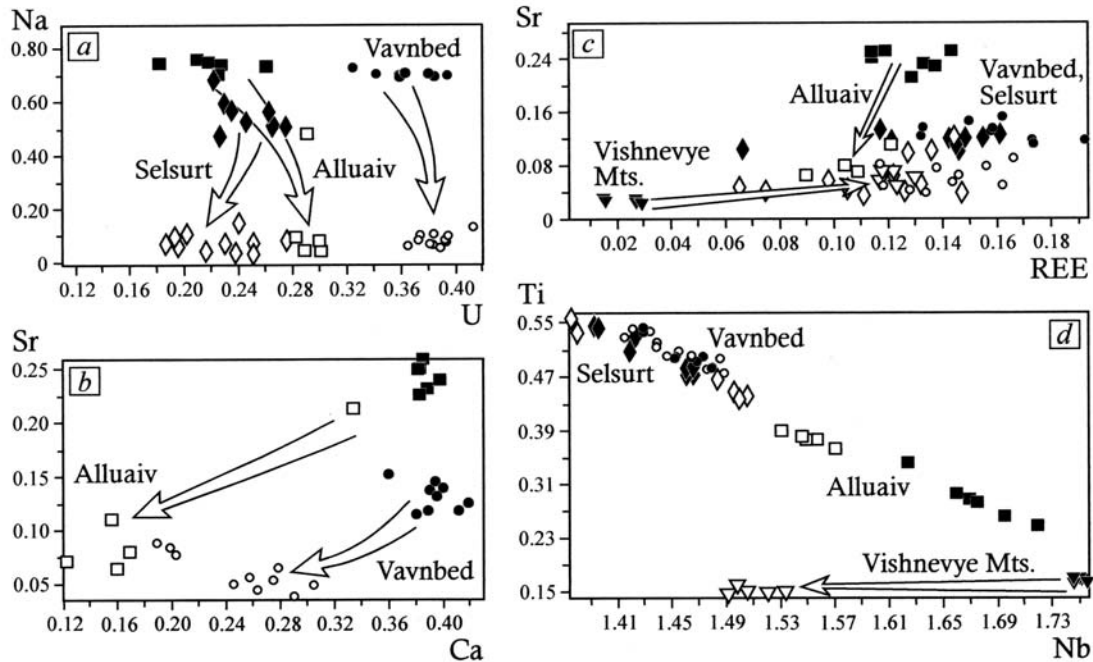


Fig. 2. Variation of selected elements (apfu) in pyrochlore-group minerals from murmanite lujavrites; data for pyrochlore from Vishnevy Gory are plotted for comparison. The compositions of uranoan pyrochlore-uranpyrochlore from Mt. Selsurt are taken from Chakhmouradian & Sitnikova (1999).

pyrochlore is typically fractured, with both linear and concentric features present (Fig. 1a).

Murmanite lujavrite LV54 contains uranoan pyrochlore profusely altered from the rim; fresh material is preserved

only in some crystals as a relic irregularly shaped core (Fig. 1b). Only the material in the core could be analyzed with confidence. Compositionally, this mineral contains moderate to high  $\text{UO}_2$  and  $\text{TiO}_2$  contents (5.0-11.0 and 6.5-

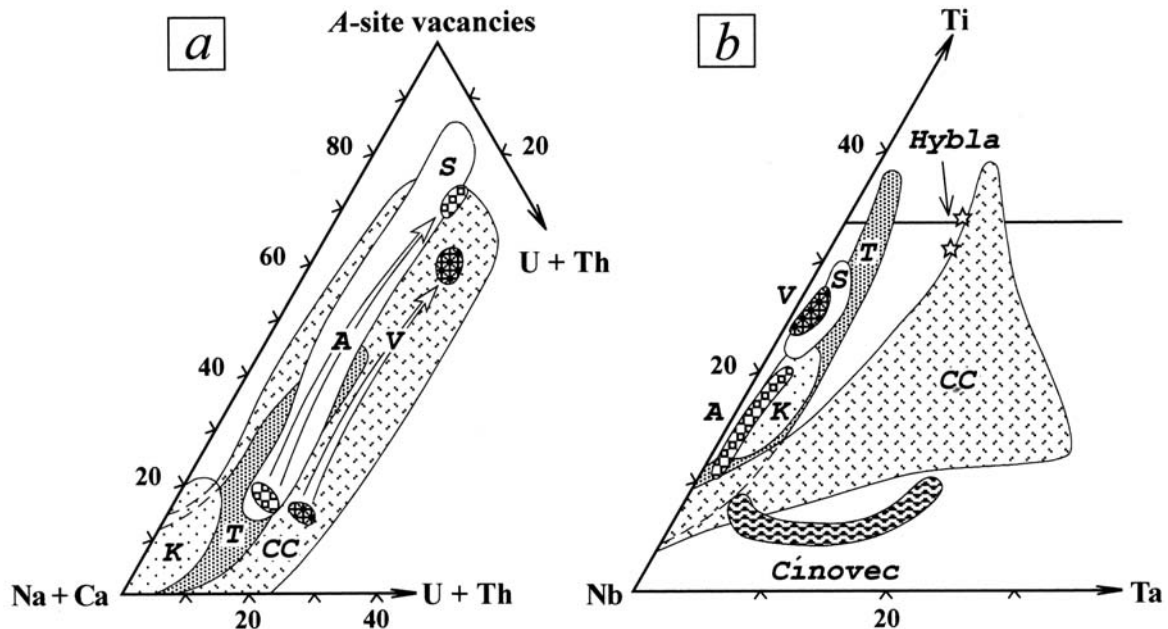


Fig. 3. Variation of major elements (at.%) in uranoan pyrochlore and uranpyrochlore from murmanite lujavrites from Mt. Alluaiv (A), Mt. Vavnbed (V) and Mt. Selsurt (S). Compositions of U-rich pyrochlore-group minerals from Khibina (K), Tuva (T), carbonatite complexes world-wide (CC), Cinovec and Hybla are plotted for comparison (data from Hogarth & Horne, 1989; Kapustin, 1989, 1991; Knudsen, 1989; Marochkina, 1990; Johan & Johan, 1994; Lumpkin & Ewing, 1995; Williams, 1996; Uher *et al.*, 1998).

Table 3. Representative compositions of pyrochlore-group minerals from metasomatic rocks.

Wt.%	pyrochlore		strontiopyrochlore		pyrochlore		plumbopyrochlore		strontio-pyrochlore				
	1	2	3	4	5	6	7	8	9	10	11	12	
Na <sub>2</sub> O	6.73	0.28	0.32	2.51	5.96	6.03	n.d	n.d	CaO	1.17	0.77	1.17	0.48
CaO	15.61	2.59	4.87	12.80	8.77	8.71	0.33	0.26	SrO	n.d	10.30	9.70	16.17
MnO	n.d	0.34	0.53	0.43	1.11	0.98	n.d	n.d	BaO	n.d	n.d	0.18	0.25
SrO	1.73	0.27	6.66	3.58	0.95	0.72	0.38	0.47	PbO	38.68	1.14	n.d	n.d
BaO	n.d	n.d	n.d	n.d	1.11	1.27	n.d	n.d	Y <sub>2</sub> O <sub>3</sub>	4.87*	n.d	n.d	n.d
PbO	n.d	n.d	n.d	n.d	n.d	n.d	36.98	37.92	La <sub>2</sub> O <sub>3</sub>	n.a	1.08	0.29	1.44
La <sub>2</sub> O <sub>3</sub>	0.63	0.72	1.53	0.57	1.87	1.68	0.45	0.71	Ce <sub>2</sub> O <sub>3</sub>	n.a	2.29	1.01	2.52
Ce <sub>2</sub> O <sub>3</sub>	1.27	2.03	2.45	1.35	2.82	3.01	1.22	1.58	UO <sub>2</sub>	n.d	0.48	n.d	n.d
Pr <sub>2</sub> O <sub>3</sub>	n.d	n.d	0.26	n.d	0.23	0.37	0.12	0.38	UO <sub>3</sub>	1.82	n.d	n.d	n.d
Nd <sub>2</sub> O <sub>3</sub>	0.66	0.47	0.82	0.33	1.01	1.06	0.06	0.17	Nb <sub>2</sub> O <sub>5</sub>	40.68	69.63	46.18	55.48
ThO <sub>2</sub>	3.56	n.d	0.39	0.20	1.55	0.55	n.d	n.d	Ta <sub>2</sub> O <sub>5</sub>	3.58	2.09	2.49	1.43
UO <sub>2</sub>	n.d	6.83	n.d	n.d	0.87	1.67	0.38	0.45	TiO <sub>2</sub>	0.81	0.49	6.26	6.68
Nb <sub>2</sub> O <sub>5</sub>	59.66	63.96	53.87	59.17	62.17	62.76	46.47	45.90	SiO <sub>2</sub>	2.82	5.88	1.74	3.66
Ta <sub>2</sub> O <sub>5</sub>	n.d	0.36	n.d	n.d	n.d	0.34	2.16	1.16	SnO <sub>2</sub>	0.61	n.a	n.a	n.a
TiO <sub>2</sub>	9.27	8.93	8.82	9.47	9.04	8.80	0.14	0.34	Fe <sub>2</sub> O <sub>3</sub>	2.87	2.07	n.d	1.37
SiO <sub>2</sub>	n.d	1.49	9.31	2.92	0.51	0.66	4.05	4.47	Al <sub>2</sub> O <sub>3</sub>	0.64	n.d	n.d	0.17
Fe <sub>2</sub> O <sub>3</sub>	0.09	0.24	1.31	0.36	0.42	0.53	1.21	1.26	Total	99.55	96.22	72.61	89.65
Total	99.21	88.51	91.14	93.69	98.39	99.14	93.95	95.07					
Structural formulae ( $\Sigma B$ -site cations = 2)													
Na	0.767	0.029	0.030	0.263	0.647	0.647	-	-	Ca	0.09	0.041	0.090	0.029
Ca	0.983	0.148	0.253	0.740	0.526	0.516	0.027	0.021	Sr	-	0.300	0.402	0.530
Mn	-	0.015	0.022	0.020	0.053	0.046	-	-	Ba	-	-	0.005	0.006
Sr	0.059	0.008	0.187	0.112	0.031	0.023	0.017	0.020	Pb	0.80	0.015	-	-
Ba	-	-	-	-	0.024	0.028	-	-	Y	0.24*	-	-	-
Pb	-	-	-	-	-	-	0.747	0.763	La	-	0.020	0.008	0.030
La	0.014	0.014	0.027	0.011	0.039	0.034	0.012	0.020	Ce	-	0.042	0.026	0.052
Ce	0.027	0.040	0.043	0.027	0.058	0.061	0.034	0.043	U	0.10	0.005	-	-
Pr	-	-	0.005	-	0.005	0.007	0.003	0.010	$\Sigma A$	1.23	0.423	0.531	0.647
Nd	0.014	0.009	0.014	0.006	0.020	0.021	0.002	0.005					
Th	0.048	-	0.004	0.002	0.020	0.007	-	-					
U	-	0.081	-	-	0.011	0.021	0.006	0.007					
$\Sigma A$	1.912	0.344	0.585	1.181	1.434	1.411	0.848	0.889	Nb	1.42	1.580	1.491	1.418
									Ta	0.07	0.029	0.049	0.022
Nb	1.586	1.546	1.180	1.443	1.572	1.570	1.576	1.552	Ti	0.05	0.018	0.336	0.284
Ta	-	0.005	-	-	-	0.005	0.044	0.024	Si	0.22	0.295	0.124	0.207
Ti	0.410	0.359	0.321	0.384	0.381	0.366	0.008	0.019	Sn	0.02	-	-	-
Si	-	0.080	0.451	0.158	0.029	0.037	0.304	0.334	Fe	0.17	0.078	-	0.058
Fe	0.004	0.010	0.048	0.015	0.018	0.022	0.068	0.071	Al	0.05	-	-	0.011
$\Sigma B$	2.000	2.000	2.000	2.000	2.000	2.000	2.000	2.000	$\Sigma B$	2.00	2.000	2.000	2.000

1-2 Core and rim of a zoned crystal, LV71; 3-4 Low-AZ sector-zoned core, and 5-6 high-AZ intermediate zones in an oscillatory-zoned crystal, LV72; 7-8 and 10 high-AZ zones in oscillatory-zoned crystals, LV79. 9 Type material, Tai Keu (Skorobogatova *et al.*, 1966); 11-12 compositions most and least enriched in Sr, Mt. Vavnbed, Lovozero (Voloshin *et al.*, 1989). \* Total content of REE dominated by Y; total of analysis 9 also includes 1.00 wt.% H<sub>2</sub>O $\pm$ ; total of analysis 11 also includes 3.59 wt.% P<sub>2</sub>O<sub>5</sub>. Total Fe expressed as Fe<sub>2</sub>O<sub>3</sub>; n.d = not detected; n.a = not analyzed.

8.3 wt.%, respectively), while being moderately enriched in Sr and REE (Table 2, anal. 7-8). The Ta<sub>2</sub>O<sub>5</sub> contents range from 1.0 to 1.5 wt.%. In texturally and modally similar sample LV53a, pyrochlore forms distinctly zoned crystals composed of uranoan pyrochlore in the core, and uranopyrochlore in the rim. The overall zoning pattern is very similar to that described above for sample LVV1, and involves a decrease in Na, Ca and Sr contents toward a hydrated rim (Fig. 2, 3). The primary uranoan pyrochlore in

sample LV53a (Table 2, anal. 9-11) has significantly higher levels of U and Sr, but lower levels of Ca and Ti in comparison with LV54. The REE and Ta contents are comparable in both samples.

Pyrochlore from albitized lujavrite LV71 forms distinctly zoned crystals with a resorbed core, discontinuous low-AZ intermediate zone, and a thin rim (Fig. 1c, d). This zoning is clearly secondary, being superposed over a primary oscillatory-type pattern discernible in most of the

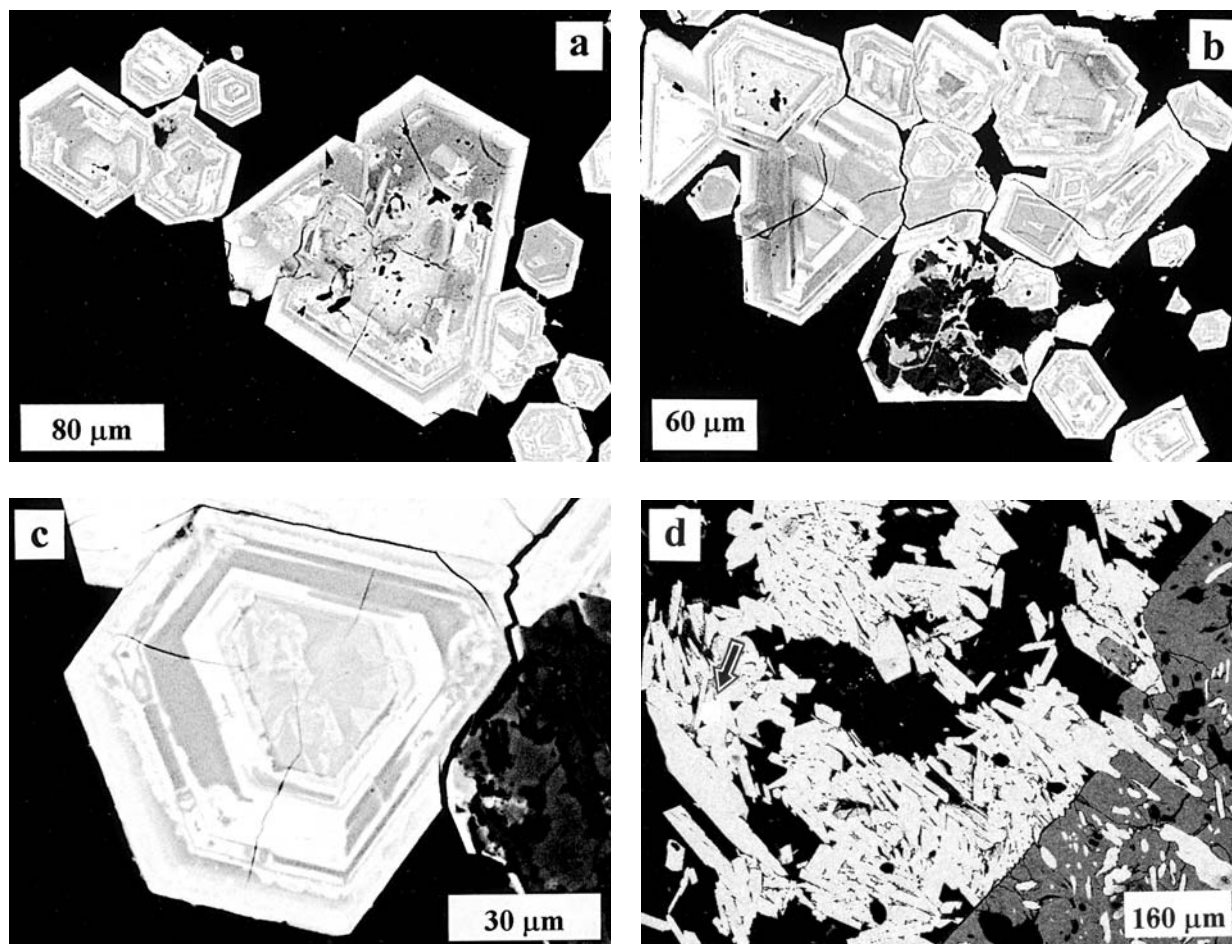


Fig. 4. Pyrochlore-group minerals from albitites, Mt. Selsurt (BSE images). (a) and (b) clusters of oscillatory-zoned pyrochlore crystals; (c) sector-zoned strontio-pyrochlore (core) successively mantled by zones with low and high Si content (white and gray, respectively); (d) plumbopyrochlore (indicated by arrow) embedded in aegirine (light gray), other minerals are narsarsukite (dark gray) and albite (black).

crystals. The intermediate zone, and less commonly, core of the crystals are strongly fractured. The fractures typically radiate from the boundary between the core and inter-

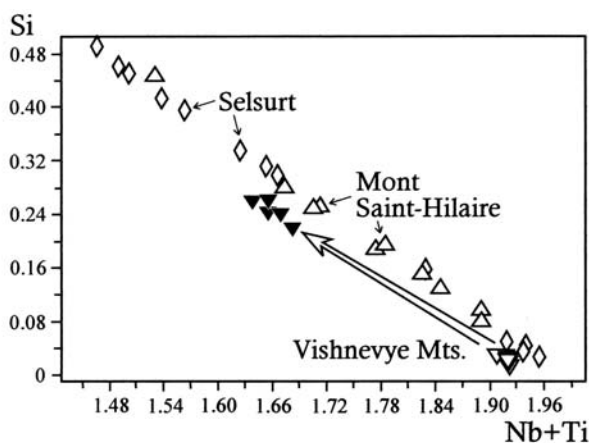


Fig. 5. Variation of Si vs. Nb (apfu) in pyrochlore from albitites (LV72); data for pyrochlore from Mont Saint-Hilaire and Vishnevy Mts. are plotted for comparison.

mediate zone outward (Fig. 1c). Compositionally, the relic core corresponds to pyrochlore enriched in CaO (14.8-15.6 wt.%) and, to lesser extent, ThO<sub>2</sub> (2.8-4.1 wt.%). The Sr and Ta contents in the core are comparable to those in the oscillatory-zoned pyrochlore from albitite (see below), but significantly lower than in pyrochlores from the murmanite lujavrites (Table 3, anal. 1). The rim of pyrochlore crystals from sample LV71 shows a high deficiency of A-site cations (ca. 82-87 %) owing to the loss of Na, Ca and Sr. In addition, the rim is strongly hydrated, silicified, and contains higher levels of U, Fe and Mn in comparison with the core (Table 3, anal. 2). Because the proportion of U in the rim outweighs those of other minor A-site elements (REE, Sr, Th and Mn), and constitutes more than 20 % of the total occupancy in this site, the rim may be formally classified as uranpyrochlore (Hogarth, 1989). The intermediate zone gives very low analysis totals (< 80 wt.%) and a very high proportion of SiO<sub>2</sub>, and was not included into Table 3.

Albitite LV72 contains abundant oscillatory-zoned crystals of pyrochlore (Fig. 4a, b). Individual zones (typically, 6-12 per crystal) vary from less than a micrometer to 10 μm in thickness, and may be continuous or fragmentary.



Table 4. Representative compositions of perovskite-group minerals from murmanite lujavrites.

Wt.%	<i>loparite-(Ce)</i> ( <i>euhedral crystals</i> )			<i>lueshite</i> ( <i>overgrowths</i> )			<i>lueshite</i> ( <i>oikocrysts</i> )					
	1	2	3	4	5	6	7	8	9	10	11	12
Na <sub>2</sub> O	8.19	9.27	9.73	11.58	12.38	13.05	13.04	13.70	13.86	14.43	12.72	13.09
CaO	3.82	2.89	2.62	1.71	1.47	1.35	1.37	0.81	0.88	0.64	0.71	0.68
SrO	4.82	4.80	2.95	2.16	2.11	2.22	2.30	3.54	3.87	2.92	3.45	2.88
La <sub>2</sub> O <sub>3</sub>	8.97	8.78	8.86	7.39	6.58	5.58	5.91	6.79	5.87	6.17	6.34	7.21
Ce <sub>2</sub> O <sub>3</sub>	17.15	15.89	15.05	11.94	9.83	8.30	8.77	7.68	6.70	6.72	8.85	9.19
Pr <sub>2</sub> O <sub>3</sub>	1.03	0.53	0.77	0.77	0.49	0.48	0.16	0.23	0.13	n.d	0.71	0.48
Nd <sub>2</sub> O <sub>3</sub>	4.57	3.57	3.35	1.94	1.47	1.23	0.93	0.92	0.74	0.27	1.42	0.84
ThO <sub>2</sub>	0.78	0.73	1.55	1.38	1.35	1.20	1.03	0.55	0.45	0.06	0.21	0.16
Nb <sub>2</sub> O <sub>5</sub>	11.92	16.96	20.30	35.30	42.24	48.07	45.30	46.93	50.42	51.91	45.93	47.50
Ta <sub>2</sub> O <sub>5</sub>	0.83	0.87	0.89	0.79	0.77	0.55	0.75	0.45	0.64	0.58	0.48	0.20
TiO <sub>2</sub>	37.70	35.45	32.94	24.44	20.89	18.83	19.68	18.48	16.84	15.57	19.39	19.20
Fe <sub>2</sub> O <sub>3</sub>	0.22	0.15	0.16	0.25	0.49	0.22	0.29	n.d	n.d	n.d	0.06	0.36
Total	100.00	99.89	99.17	99.65	100.07	101.08	99.53	100.08	100.40	99.27	100.27	101.79
Structural formulae to 3 atoms of oxygen												
Na	0.460	0.517	0.548	0.644	0.681	0.704	0.714	0.750	0.754	0.791	0.697	0.705
Ca	0.119	0.089	0.082	0.053	0.045	0.040	0.041	0.025	0.026	0.019	0.021	0.020
Sr	0.081	0.080	0.050	0.036	0.035	0.036	0.038	0.058	0.063	0.048	0.057	0.046
La	0.096	0.093	0.095	0.078	0.069	0.057	0.062	0.071	0.061	0.064	0.066	0.074
Ce	0.182	0.167	0.160	0.125	0.102	0.085	0.091	0.079	0.069	0.070	0.092	0.093
Pr	0.011	0.006	0.008	0.008	0.005	0.005	0.002	0.002	0.001	-	0.007	0.005
Nd	0.047	0.037	0.035	0.006	0.015	0.012	0.009	0.009	0.007	0.003	0.014	0.008
Th	0.005	0.005	0.010	0.009	0.009	0.008	0.007	0.004	0.003	-	0.001	0.001
ΣA	1.001	0.994	0.988	0.974	0.961	0.947	0.964	0.998	0.984	0.995	0.955	0.952
Nb	0.156	0.221	0.267	0.458	0.542	0.605	0.578	0.599	0.639	0.663	0.587	0.596
Ta	0.007	0.007	0.007	0.006	0.006	0.004	0.006	0.003	0.005	0.004	0.004	0.002
Ti	0.821	0.767	0.719	0.528	0.446	0.394	0.418	0.393	0.355	0.331	0.412	0.401
Fe	0.005	0.003	0.003	0.005	0.010	0.005	0.006	-	-	-	0.001	0.008
ΣB	0.989	0.998	0.996	0.997	1.004	1.008	1.008	0.995	0.999	0.998	1.004	1.007

1-7 LV54; 8-10 LV18; 11-12 LVE1. Total Fe expressed as Fe<sub>2</sub>O<sub>3</sub>; n.d = not detected.

The low-AZ zones are depleted in Na and Ca, but enriched in Si, Fe, Mn, Sr and H<sub>2</sub>O relative to the brighter zones. Some crystals have a core with a distinct sectorial zoning (Fig. 4c). The relatively low-AZ sectors (strontiopyrochlore) are depleted in Na, Ca and Nb, and enriched in Sr, REE and Si in comparison with the higher-AZ areas (Table 3, anal. 3-4). The Si content shows a negative correlation with the total (Nb+Ti) content throughout successive zones with a different AZ (Fig. 5). The highest SiO<sub>2</sub> and Fe<sub>2</sub>O<sub>3</sub> contents observed in this sample (16.8 and 2.2 wt.%, respectively) are invariably associated with the low-AZ zones having the highest levels of H<sub>2</sub>O (analysis totals < 85 wt.%). Intragranular variation in other minor components is insignificant. The U, Sr and Ta contents in the fresh pyrochlore (high-AZ areas) are noticeably lower than in the U-bearing pyrochlore from the murmanite lujavrites, whereas the REE contents are comparable in pyrochlore from the two rock types.

Samples of albitite LV79 (Fig. 4d) contain abundant plumbopyrochlore (up to 37.9 wt.% PbO) and strontiopyrochlore (up to 10.3 wt.% SrO), commonly in spatial proximity. Both minerals are strongly altered, and exhibit weak

oscillatory-type zoning. Zones with comparatively higher AZ have lower SiO<sub>2</sub> and Fe<sub>2</sub>O<sub>3</sub> contents, and higher analysis totals; hence, they are deemed less altered than the low-AZ areas. In Table 3, we included the analytical data only for the high-AZ zones (anal. 7-8 and 10).

### Perovskite-group minerals

Murmanite lujavrite LV54 contains abundant euhedral, inclusion-free crystals of niobian calcian loparite-(Ce) (for the nomenclature of perovskite-group minerals, see Mitchell, 1996). The mineral displays a significant intragranular variation in composition involving an increase in Na and Nb, and concomitant decrease in REE, Ti, Ca and Sr toward the rim (Table 4, anal. 1-3). Locally, the crystals exhibit a discontinuous "fringe" composed of subhedral lueshite. From the early crystals of loparite-(Ce) to the lueshite overgrowths, there is a continuous series of compositions that plot almost parallel to the Na<sub>1/2</sub>REE<sub>1/2</sub>TiO<sub>3</sub>-NaNbO<sub>3</sub> join (Fig. 6). In this sample, lueshite also occurs as oikocrysts up to 250 μm across. The composition of oikocrysts approaches that of the most Na-

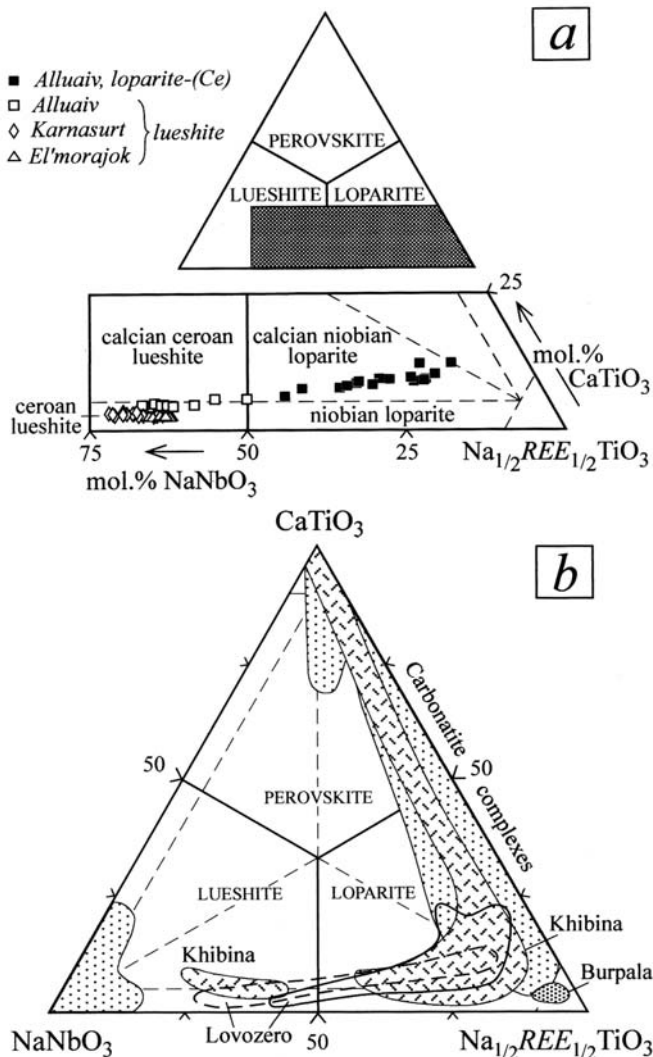


Fig. 6. Compositional variation (mol.%) of perovskite-group minerals from murmanite lujavrites. (a) Individual samples; (b) overall compositional variation (dashed line) in comparison with the evolutionary trend of perovskite-group minerals from intrusive series (2)-(4) at Lovozero (solid line: Mitchell & Chakhmouradian, 1996), and from other alkaline complexes (shaded fields: Chakhmouradian & Mitchell, 1998; Chakhmouradian *et al.*, 1999).

and Nb-rich lueshite from the “fringes” (*cf.* Table 4, anals. 6 and 7). Similar lueshite oikocrysts are found in murmanite lujavrites LV18 and LVE1 (Fig. 7 a-c, Table 4). In the ternary  $\text{Na}_{1/2}\text{REE}_{1/2}\text{TiO}_3$ - $\text{NaNbO}_3$ - $\text{CaTiO}_3$  (- $\text{SrTiO}_3$ ) diagram, all oikocryst compositions cluster between 60 and 70 mol.%  $\text{NaNbO}_3$  in the field of ceroan lueshite (Fig. 6a). Textural evidence indicates that this lueshite formed after the bulk of the rock, but prior to the crystallization of oikocrysts of “agpaitic” silicates, *i.e.*, murmanite, lamprophyllite and alkali amphibole (Fig. 7). In sample LV54, where lueshite co-exists with pyrochlore, the latter mineral clearly preceded the former. In contrast, pyrochlore from hydrothermal and metasomatic alkaline parageneses is commonly observed to replace a perovskite-group precursor (Semenov *et al.*, 1968; Voloshin *et al.*, 1989).

## Discussion

### Occurrence and composition of niobate minerals in agpaitic alkaline rocks

Although niobate minerals are ubiquitous in nepheline-syenite complexes, there is a paucity of data on their distribution and chemistry. Pyrochlore is a common accessory phase in miaskitic mineral parageneses, whereas in a more alkali-rich environment, the major Nb oxide is typically a member of the perovskite group. Mitchell & Chakhmouradian (1996), and Chakhmouradian & Mitchell (1998) have demonstrated that in sodic agpaitic rocks, the overall evolutionary trend of perovskite-group minerals is from calcian niobian loparite-(Ce) to ceroan lueshite or isolueshite at low to moderate contents of the  $\text{SrTiO}_3$  end-member (Fig. 6b). This trend is expressed both on a macro-scale (*i.e.*, toward younger intrusive series) and micro-scale (zoning). The previous studies of perovskite-group minerals from Lovozero focused on the most volumetrically significant petrographic units, *i.e.*, series 3 and 4 (Ifantopulo & Osokin, 1979; Kogarko *et al.*, 1996), and 2 through 4 (Mitchell & Chakhmouradian, 1996). Prior to our work, perovskite-group minerals had not been described from the murmanite lujavrites (series 5). The compositional data obtained in this work (Fig. 6) are in excellent agreement with the trend established for the Lovozero intrusion by Mitchell & Chakhmouradian (1996). The overall trend is mimicked by the core-to-rim zoning pattern in loparite-(Ce) from sample LV54. The presence of lueshite oikocrysts distinguishes the murmanite lujavrites from the other intrusive series, suggesting that the former crystallized from the most evolved portions of phonolitic magma.

In a number of studies, “pyrochlore” has been identified as a part of agpaitic parageneses (*e.g.*, Wallace *et al.*, 1990). Complete compositional data (including such elements as Ta, U, Th, Sr, REE and Pb) for these minerals are typically unavailable, and hence, their accurate identification is not possible. In some cases, the presence of unaccounted-for elements can be readily inferred from low analysis totals. For comparative purposes, we examined several samples of pyrochlore-group minerals from alkaline parageneses relevant to our study. Their provenance and mineral compositions are described in Table 5; representative compositions of pyrochlore-group phases from these samples are given in Table 6.

Analysis of our data and those available in the literature shows that pyrochlore-group minerals from agpaitic rocks most typically form during the final evolutionary stages characterized by the appearance of subsolidus “sugary” or platy albite, green fibrous aegirine and natrolite in the mineral assemblage (Kostyleva-Labuntsova *et al.*, 1978; Kapustin, 1989, 1991). Here, crystallization of pyrochlore (*sensu lato*) is related to interaction of the primary mineral paragenesis (alkali feldspar, nepheline, prismatic aegirine or aegirine-augite, alkali amphiboles) with a deuteric or metasomatic fluid. It remains debatable whether the Nb, Ti and rare elements sequestered in pyrochlore are derived from a primary host, *e.g.*, loparite, titano- and niobosili-

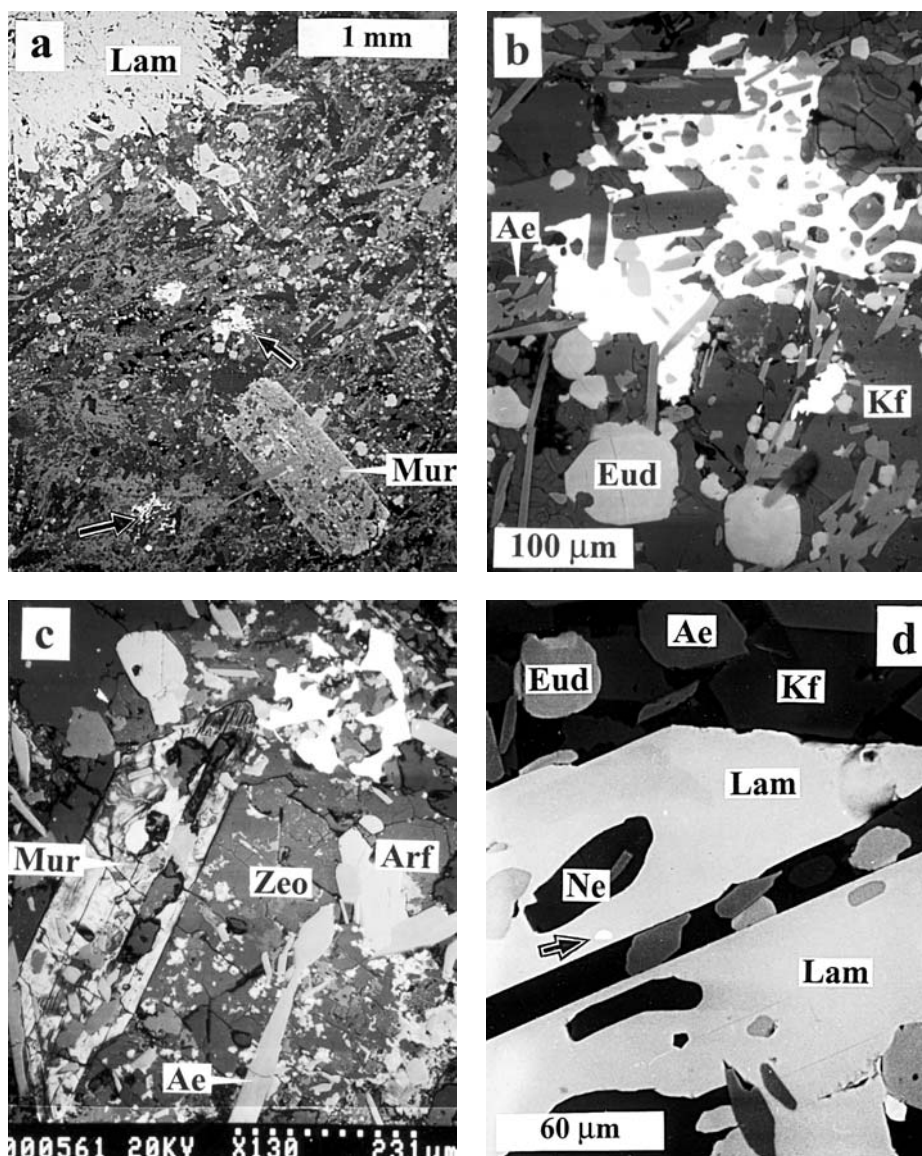


Fig. 7. Perovskite-group minerals from murmanite lujavrites (BSE images). (a) Pseudoporphyritic texture defined by the presence of oikocrysts of murmanite (Mur), lamprophyllite (Lam) and lueshite (white grains indicated by arrows), Mt. Karnasurt; (b) detail of (a), note chadacrysts of aegirine (Ae), potassium feldspar (Kf) and eudialyte (Eud) in lueshite (white); (c) oikocrysts of lueshite (white) and murmanite (Mur) in a zeolitized mesostasis (Zeo), other minerals are arfvedsonite (Arf) and aegirine (Ae), El'morajok Valley; (d) inclusions of lueshite (white) in oikocrystic lamprophyllite (Lam), other minerals are aegirine (Ae), nepheline (Ne), potassium feldspar (Kf) and eudialyte (Eud), Mt. Karnasurt.

cates (Kostyleva-Labuntsova *et al.*, 1978), or from a late-stage fluid. Only in rare cases where pyrochlore-group phases are observed to directly replace a primary Ti-Nb host, *e.g.*, lueshite or loparite-(Ce), can the source of these elements be unambiguously established (Semenov *et al.*, 1968; Voloshin & Polezhaeva, 1979). Kapustin (1989) suggested that dissolution of astrophyllite, rinkite and strontian apatite during albitization of agpaite pegmatites at Khibina (Kola Peninsula) could provide the amount of Ti, REE and Sr necessary for the crystallization of pyrochlore, although Nb and Ta were, at least, partly derived from an "extrinsic" source. In albitized nepheline syenites and pegmatites, pyrochlore is commonly found in

a mineral assemblage characteristic of miaskitic rocks, *i.e.*, with zircon, biotite, ilmenite, titanite and apatite, attesting to a decrease in alkalinity during the terminal evolutionary stages. The sample of eudialyte lujavrite (LVE2) examined in this study provides a good example of such late-stage pyrochlore crystallization.

In albitites and related albite-rich metasomatic assemblages, pyrochlore is a relatively common accessory mineral, as demonstrated in this work and several earlier publications (*e.g.*, Voloshin *et al.*, 1989; Kapustin, 1991). The composition of pyrochlore-group minerals from metasomatic rocks is very variable. Examples include *bona fide* pyrochlore, plumbopyrochlore and strontio-pyrochlore from

Table 5. Details on selected occurrences of pyrochlore-group minerals.

Locality	Rock type	Associated minerals	References
Vishnevye Mts. Middle Urals, Russia	Miaskitic nepheline syenite cross-cut by calcite carbonatite	Ne, Af, oligoclase, biotite, cancrinite, zircon, ilmenite, apatite	Kogarko <i>et al.</i> (1995)
Pegmatite Peak Bearpaw Mts., Montana, USA	Nepheline-syenitic pegmatite	Ne, Mc, Ae, Lam, Tit, biotite, ilmenite, chevkinite, zircon, thorite, loparite-(Ce)	Chakhmouradian & Mitchell (1999)
Mont Saint-Hilaire Québec, Canada	Nepheline-syenitic pegmatite	Niobian ilmenite, pyrrhotite, rhodochrosite, rutile, manganocolumbite	Horváth & Gault (1990)
Dara-i-Pioz Garm district, Tajikistan	Quartz-albite-aegirine rock developed after alkali syenite	Ab, Ae, quartz, Mc, miserite, apatite, tadzhikite, stillwellite	Requir <i>et al.</i> (1999)
Mt. Niorkpakhk Khibina, Kola Peninsula, Russia	Albitite developed after nepheline syenite	Ab, Ae, Mc (relict), Eud, astrophyllite, loparite-(Ce), galena	this work

Mineral symbols as in Table 1.

Lovozero (this work, Voloshin *et al.*, 1989), plumbopyrochlore from Tai Keu (Skorobogatova *et al.*, 1966), ceroan pyrochlore from Korgeredaba (Kapustin, 1991), uranoan pyrochlore from Dara-i-Pioz and uranpyrochlore from Khibina (see Tables 3 and 5 for representative compositions). Prior to our study, plumbopyrochlore had not been encountered at Lovozero; a few known occurrences of this mineral include laterites of the Araxá carbonatite complex in Brazil (Mariano *et al.*, 1997), Oka carbonatites in Québec (Hogarth, 1989), and granitic pegmatites of the Kola Peninsula (Voloshin *et al.*, 1981). Plumbobetafite, a closely related species with  $Nb > Ti$  (but  $Nb < 2Ti$ ), was described from a microcline-quartz-albite-aegirine-riebeckitic rock cross-cutting nepheline syenite at the Burpala alkaline complex, Siberia (Ganzeev *et al.*, 1969), and from granitic pegmatites of the Kola Peninsula (Voloshin *et al.*, 1993). The compositional diversity of pyrochlore from albitites is not surprising, as these rocks form in a broad range of  $P$ - $T$  conditions, and various petrographic settings, including felsic metamorphic rocks, alkali granites and syenites, miaskitic and agpaitic feldspathoid syenites.

The data obtained in the present study show that in peralkaline rocks, pyrochlore-group phases may form early in the crystallization history, prior to such characteristic "agpaitic" minerals as loparite-(Ce), lueshite, eudialyte, murmanite and lamprophyllite. This observation is also consistent with the occurrence of betafite ( $Nb \approx Ti$ ) in nepheline-syenitic pegmatites of Bearpaw Mountains (Chakhmouradian & Mitchell, 1999). Crystallization of pyrochlore or betafite in agpaitic rocks may be favored by initially low activities of alkalis and silica in the magma, or by enrichment of this magma in elements more readily accommodated in the pyrochlore structure than in such alternative hosts as loparite. Whereas the paragenesis of

betafite in the Bearpaw pegmatites is clearly "miaskitic" in character (*ibid.*), pyrochlore-group minerals from the murmanite lujavrites (LVV1, LV54, LV53a) are not associated with minerals that would suggest low alkalinity of magma during the early crystallization stage. However, pyrochlore from the Lovozero murmanite lujavrites is characteristically enriched in U (5.0-26.4 wt.%  $UO_2$ ), the element not readily accommodated in a perovskite-type structure because of its small ionic radius. Note that the recently described pyrochlore from an agpaitic pegmatite at Mt. Karnasurt (Zadov *et al.*, 1999), as well as the Bearpaw betafite also contain elevated levels of U (up to 16.8 and 8.8 wt.%  $UO_2$ , respectively).

U-rich members of the pyrochlore family occur in a variety of parageneses, including granitic pegmatites (Prašivá, Slovakia: Uher *et al.*, 1998), fenitized granitic pegmatites (Ulanerginskii complex, Tuva: Kapustin, 1991), evolved granites (Massif Central, France: Ohnenstetter & Piantone, 1992, and Cínovec, Czech Republic: Johan & Johan, 1994), phoscorites and carbonatites (*e.g.*, Fort Portal, Uganda: Hogarth & Horne, 1989). In contrast to the uranpyrochlore and uranoan pyrochlore from Lovozero (Table 2, Fig. 3b), pyrochlore-group minerals from granitic rocks (Ohnenstetter & Piantone, 1992; Johan & Johan, 1994; Uher *et al.*, 1998) are invariably enriched in Ta (> 2.8 wt.%  $Ta_2O_5$ , with some compositions corresponding to uranmicrolite), and contain appreciable levels of W and Sn (up to 6.5 wt.%  $WO_3$  and 1.4 wt.%  $SnO_2$ ). Betafite and uranpyrochlore from carbonatitic assemblages show a wide variation in Ta/Nb ratio, but characteristically lack detectable W and Sn. In addition, U-rich pyrochlore-group minerals from carbonatites and granitic rocks contain significantly lower levels of Sr and light REE, in comparison with their counterparts from agpaitic rocks.

Table 6. Representative compositions of pyrochlore-group minerals from other localities.

Wt.%	Vishnevye Mts.		Pegmatite Peak		Mont Saint-Hilaire			Dara-i Pioz	Khibina		
	1	2	3	4	5	6	7	8	9		
Na <sub>2</sub> O	6.44	4.32	Na <sub>2</sub> O	4.15	3.35	9.43	8.71	10.82	4.53	Na <sub>2</sub> O	n.d
K <sub>2</sub> O	n.d	0.45	CaO	7.55	7.11	10.89	10.32	11.64	12.09	CaO	3.94
CaO	15.44	9.24	MnO	n.d	n.d	n.d	n.d	n.d	n.d	MnO	0.81
MnO	0.17	0.23	SrO	0.83	0.46	0.39	0.45	n.d	1.81	SrO	0.59
SrO	0.76	3.67	La <sub>2</sub> O <sub>3</sub>	0.89	0.33	0.49	0.11	n.d	n.d	La <sub>2</sub> O <sub>3</sub>	0.31
Y <sub>2</sub> O <sub>3</sub>	n.d	0.31	Ce <sub>2</sub> O <sub>3</sub>	7.40	7.02	1.09	1.01	0.49	n.d	Ce <sub>2</sub> O <sub>3</sub>	1.97
La <sub>2</sub> O <sub>3</sub>	0.14	0.59	Pr <sub>2</sub> O <sub>3</sub>	1.21	0.95	n.d	n.d	n.d	n.d	Pr <sub>2</sub> O <sub>3</sub>	n.d
Ce <sub>2</sub> O <sub>3</sub>	0.43	1.15	Nd <sub>2</sub> O <sub>3</sub>	3.60	3.59	0.75	0.34	n.d	n.d	Nd <sub>2</sub> O <sub>3</sub>	n.d
Nd <sub>2</sub> O <sub>3</sub>	0.17	0.42	ThO <sub>2</sub>	16.49	18.97	0.94	1.02	n.d	n.d	ThO <sub>2</sub>	n.d
ThO <sub>2</sub>	1.26	1.65	UO <sub>2</sub>	4.72	8.80	n.d	n.d	n.d	23.37	UO <sub>2</sub>	46.20
Nb <sub>2</sub> O <sub>5</sub>	64.48	58.10	Nb <sub>2</sub> O <sub>5</sub>	33.54	26.58	64.87	64.25	57.27	47.96	Nb <sub>2</sub> O <sub>5</sub>	25.11
Ta <sub>2</sub> O <sub>5</sub>	3.71	3.81	Ta <sub>2</sub> O <sub>5</sub>	1.31	1.23	0.63	1.05	0.79	1.08	Ta <sub>2</sub> O <sub>5</sub>	0.93
TiO <sub>2</sub>	3.72	3.40	TiO <sub>2</sub>	15.38	19.19	4.34	3.01	3.79	7.85	TiO <sub>2</sub>	4.76
SiO <sub>2</sub>	0.34	4.16	SiO <sub>2</sub>	1.66	1.54	1.67	3.35	8.39	0.24	SiO <sub>2</sub>	6.10
Fe <sub>2</sub> O <sub>3</sub>	0.01	n.d	Fe <sub>2</sub> O <sub>3</sub>	0.48	0.51	0.12	0.40	0.32	0.26	Fe <sub>2</sub> O <sub>3</sub>	0.41
Al <sub>2</sub> O <sub>3</sub>	n.d	0.44	F	n.a	n.a	0.58	0.16	0.31	n.a	Al <sub>2</sub> O <sub>3</sub>	1.82
Total	97.07	91.94	Total	99.21	99.63	95.95*	94.11*	93.69*	99.18	Total	92.95
Structural formulae ( $\Sigma B$ -site cations = 2)											
Na	0.750	0.485	Na	0.553	0.453	1.059	0.958	1.116	0.620	Na	-
K	-	0.033	Ca	0.556	0.531	0.676	0.627	0.664	0.915	Ca	0.356
Ca	0.993	0.573	Mn	-	-	-	-	-	-	Mn	0.058
Mn	0.009	0.011	Sr	0.033	0.019	0.013	0.015	-	0.074	Sr	0.029
Sr	0.026	0.123	La	0.023	0.008	0.010	0.002	-	-	La	0.010
Y	-	0.010	Ce	0.186	0.179	0.023	0.021	0.010	-	Ce	0.061
La	0.003	0.013	Pr	0.030	0.024	-	-	-	-	Pr	-
Ce	0.009	0.024	Nd	0.088	0.089	0.016	0.007	-	-	Nd	-
Nd	0.004	0.010	Th	0.258	0.301	0.012	0.013	-	-	Th	-
Th	0.017	0.022	U	0.072	0.136	-	-	-	0.367	U	0.866
$\Sigma A$	1.811	1.304	$\Sigma A$	1.799	1.740	1.809	1.643	1.789	1.976	$\Sigma A$	1.380
Nb	1.751	1.521	Nb	1.042	0.837	1.699	1.648	1.378	1.532	Nb	0.956
Ta	0.061	0.060	Ta	0.024	0.023	0.010	0.016	0.011	0.021	Ta	0.021
Ti	0.168	0.148	Ti	0.795	1.006	0.189	0.129	0.152	0.416	Ti	0.302
Si	0.020	0.241	Si	0.114	0.107	0.097	0.190	0.446	0.017	Si	0.514
Fe	-	-	Fe	0.025	0.027	0.005	0.017	0.013	0.014	Fe	0.026
Al	-	0.030	$\Sigma B$	2.000	2.000	2.000	2.000	2.000	2.000	Al	0.181
$\Sigma B$	2.000	2.000	F	-	-	0.106	0.029	0.052	-	$\Sigma B$	2.000

1 Core and 2 rim of a zoned pyrochlore crystal; 3-4 betafite inclusion in loparite-(Ce); 5-7 zones with progressively decreasing AZ in an oscillatory-zoned pyrochlore crystal; 8 unzoned crystal of uranoan pyrochlore; 9 high-AZ area in a profusely altered crystal of uranpyrochlore. \* Analysis totals include less O = F<sub>2</sub>. Total Fe expressed as Fe<sub>2</sub>O<sub>3</sub>; n.d = not detected; n.a = not analyzed.

### Alteration patterns in pyrochlore crystals

Crystals of uranoan pyrochlore from murmanite lujavrites invariably show profuse alteration involving a decrease in Na, Ca and Sr contents from the core outwards (Fig. 2a, b). The proportion of relatively higher-charged cations (U and REE) does not change or only slightly diminishes toward the rim (Fig. 2a, c). These changes are accompanied by increasing cation deficiency in the A site (Fig. 3a) and progressive hydration. Fresh uranoan pyrochlore preserved in the core of some crystals shows

only minor cation deficiency (< 0.20-0.35 atoms per formula unit), whereas the uranpyrochlore rim typically has from 50-65 % of A-site vacancies ( $x = 1.0-1.3$ ). The total positive charge created by the A- and B-site cations in the deficient uranpyrochlore does not exceed +12.3 (as opposed to the ideal value of +13.0), indicating that a significant proportion of anions in the Y site (OH+F+O) was also removed by leaching. The H<sub>2</sub>O contents estimated from  $x$  for the most A- and Y-site deficient varieties (Table 2, anal. 6 and 11) are about 6.3 and 7.7 wt.%, which agrees well with the values calculated by difference of analysis

totals to 100 % (6.3 and 8.9 wt.%, respectively). The extent of alteration observed in this pyrochlore (Fig. 3) is comparable to that produced by secondary processes in pyrochlore from miaskitic rocks at Brevik, Norway (Lumpkin & Ewing, 1995). However, the murmanite-lujavrite samples examined in the present study are fresh, and lack any evidence of extensive supergene alteration (e.g., replacement of nepheline by gibbsite). Therefore, the processes of ion leaching and hydration undoubtedly resulted from interaction of the primary uranoan pyrochlore with a deuteric fluid, in a manner similar to the replacement of loparite by "metaloparite" under decreasing temperature, pH and  $a(\text{Na}^{1+})$  (Chakhmouradian *et al.*, 1999).

For comparison, we also studied the alteration pattern exhibited by pyrochlore from the miaskitic nepheline syenites of the Vishnevye Mountains. In common with the Lovozero material, this pyrochlore is zoned toward Na- and Ca-depleted compositions at the rim. However, the proportion of larger and higher-charged cations (K, Sr, REE and Th) increases noticeably toward the rim of the crystals (Fig. 2c, Table 6). These changes are accompanied by a dramatic increase in Si content coupled with depletion in Nb (Fig. 2d). This cation-exchange pattern and the moderate extent of alteration distinguish this pyrochlore from that in the Lovozero lujavrites, but are similar to the transitional alteration of pyrochlore from an unspecified locality at Langesundfjord (Norway), as described by Lumpkin & Ewing (1995). Unfortunately, the description provided for the Langesundfjord material is insufficient to conclude whether it originates from a miaskitic or an apgaitic paragenesis. The relatively high CaO and low SrO contents in the primary pyrochlore from this locality (*ibid.*, Table 2) suggest a miaskitic source (*cf.* 15.1-15.9 wt.% CaO and 0.7-0.9 wt.% SrO in the Vishnevye material; 4.6-11.0 wt.% CaO and 2.6-7.2 wt.% SrO in the uranoan pyrochlore from Lovozero).

The pyrochlore crystals from albitites show essentially two types of alteration: patchy, confined to the rim (Fig. 1c, d), and regular, conformable with oscillatory zoning (Fig. 4 a-c). Both these types involve ion leaching, hydration and enrichment of the altered material in Si, Fe and Mn (Table 3). Whereas the patchy pattern of alteration is clearly secondary, the regular type may have developed *simultaneously* with crystallization due to oscillation of pH,  $a(\text{SiO}_2)$ ,  $a(\text{Na}^{1+})$ ,  $a(\text{Ca}^{2+})$  and activities of the minor components in a layer adjacent to the growing crystal. Note that variations in pH alone are probably capable of changing the solubility of silica and cations in the metasomatic fluid, and causing the observed zoning pattern. The lack of linkage between successive low-AZ zones, and the absence of alteration along fractures (Fig. 4 a-c) further testify against the secondary (post-crystallization) nature of this type of alteration. Crystals of pyrochlore from Mont Saint-Hilaire show a similar type of oscillatory zoning.

### Structural role of silicon in pyrochlore

The position of Si in the pyrochlore structure is uncertain. Hogarth (1989) noted that the high amounts of Si

reported to substitute for Nb in the *B* site of some pyrochlores should be treated with caution. Elevated silica contents typically occur in pyrochlore-group minerals with a high proportion of vacancies in the *A*-site, *i.e.*, U- and Th-bearing pyrochlore, betafite, strontio-pyrochlore, plumbopyrochlore, *etc.* (e.g., Uher *et al.*, 1998). Pyrochlore-type phases with Si in the octahedral site are well known among synthetic compounds (Reid *et al.*, 1977). According to Voloshin *et al.* (1989), the crystal structure of strontio-pyrochlore from Lovozero could not be satisfactorily refined assuming that Si or P enters the *B* site ( $\text{SiO}_2$  and  $\text{P}_2\text{O}_5$  contents in their samples range from 1.7-3.7 and 0-7.0 wt.%, respectively). Infrared spectra of this mineral exhibit a series of absorption bands indicative of  $(\text{SiO}_4)$  and  $(\text{PO}_4)$ . Accordingly, Voloshin *et al.* (1989) suggest that the impurities of Si and P in strontio-pyrochlore are not structurally bound, but instead occur "in an amorphous or dispersed state" (translation ours). Unfortunately, the nature of a Si-P host in this mineral could not be further ascertained.

Alternatively, silicified varieties of pyrochlore may represent submicroscopic intergrowths of altered precursor with komarovite,  $(\text{H,Ca,Na})_2(\text{Nb,Ti})_2\text{Si}_2\text{O}_{10}(\text{OH,F})_2$ , whose structure is related to that of pyrochlore (Krivokoneva *et al.*, 1979). Replacement of pyrochlore by "macroscopic" komarovite was actually observed in alkaline pegmatites of the Ilímaussaq complex in Greenland (*ibid.*). Importantly, neither the presence of absorbed amorphous silica nor intergrowths with komarovite could explain the antipathetic correlation between the Si and (Nb+Ti) contents observed in the present study (Fig. 5). In addition, the existence of a hypothetical silica-rich impurity is contradicted by the enrichment in Si being confined to discrete zones in an overall zoning pattern, or sectorial variation in Si/Nb ratio (Fig. 4 a-c). At present, the form of silica occurrence in pyrochlore remains enigmatic, and transmission-electron microscopy studies (TEM) of homogeneous crystalline material are clearly required to resolve this problem. The "silicified" pyrochlores from Lovozero exhibit significant micro-scale variations in Si content and, hence, are unsuitable for this purpose. Previous attempts to ascertain the structural position of Si in a similar material by TEM were unsuccessful (Voloshin *et al.*, 1989). Note that examination of such pyrochlores by TEM is not trivial, and, in addition to compositional heterogeneity, is hampered by the commonly metamict nature of these phases and their instability under the electron beam.

### Conclusions

At Lovozero, the evolutionary trend exhibited by perovskite-group minerals from the intrusive rocks culminates with the appearance of ceroan lueshite in the murmanite lujavrites. This mineral occurs as overgrowths on earlier-crystallized loparite-(Ce) and, more commonly, as discrete oikocrysts. Lueshite formed prior to oikocrystic titanosilicates (murmanite, lamprophyllite, *etc.*), but subsequent to pyrochlore. Pyrochlore from the murmanite lujavrites is enriched in U and, to lesser extent, Sr and REE. Given that the samples described by Chakhmouradian &

Sitnikova (1999) and in the present work were collected many kilometers apart, the enrichment in U appears to be a characteristic compositional signature of pyrochlore from petrographic series (5). Subsolvus re-equilibration resulted in ionic leaching from and hydration of the primary uranoan pyrochlore and its replacement by cation-deficient uranopyrochlore. This process, involving interaction of the early mineral paragenesis with a deuteric fluid under decreasing pH and temperature, appears to be an important component of the evolutionary history of agpaite rocks (see also Chakhmouradian & Mitchell, 1999, 2002). Crystallization of the perovskite- and pyrochlore-group niobates in the murmanite-lujavrites indicates that these rocks formed from the most evolved portions of phonolitic magma.

Albite-rich metasomatic rocks from Lovozero typically contain "silicified" varieties of pyrochlore with an oscillatory zoning pattern and, in some cases, superimposed patchy (irregular) zoning. Compositionally, the metasomatic pyrochlore ranges from nearly stoichiometric Na-Ca-rich compositions to strongly cation-deficient strontio-pyrochlore and plumbopyrochlore. The oscillatory zoning pattern observed involves significant variation in cation occupancy of the A-site (primarily Na, Ca and Sr), as well as in the Si content which correlates antipathetically with (Nb+Ti). This pattern is believed to result from oscillations in pH and the activities of major components throughout the crystallization history of pyrochlore; *i.e.*, growth episodes followed by episodes of compositional re-equilibration with a metasomatic fluid.

**Acknowledgements:** This work was supported by the Natural Sciences and Engineering Research Council of Canada. We gratefully acknowledge the help of Anne Hammond and Allan MacKenzie with sample preparation and analytical work, respectively. Henning Sørensen, Tom Andersen and an anonymous referee are thanked for their constructive and stimulating criticism.

## References

- Borutskii, B.E. (1988): Rock-forming minerals of hyperagpaite complexes. Nauka Press, Moscow, 215 p. (in Russ.).
- Bussen, I.V. & Sakharov, A.S. (1972): Petrology of the Lovozero alkaline massif. Nauka Press, Moscow, 296 p. (in Russ.).
- Chakhmouradian, A.R. & Mitchell, R.H. (1998): Compositional variation of perovskite-group minerals from the Khibina Complex, Kola Peninsula, Russia. *Can. Mineral.*, **36**, 953-970.
- , — (1999): Primary, agpaite and deuteric stages in the evolution of accessory Sr, REE, Ba and Nb- mineralization in nepheline-syenite pegmatites at Pegmatite Peak, Bearpaw Mts, Montana. *Mineral. Petrol.*, **67**, 85-110.
- , — (2002): The mineralogy of Ba- and Zr-rich alkaline pegmatites from Gordon Butte, Crazy Mountains (Montana, USA): Comparisons between potassic and sodic agpaite pegmatites. *Contrib. Mineral. Petrol.*, **143**, 93-114.
- Chakhmouradian, A.R. & Sitnikova, M.A. (1999): Radioactive minerals in murmanite-lorenzenite tinguaitite at Mt. Selsurt, Lovozero complex, Kola Peninsula. *Eur. J. Mineral.*, **11**, 871-878.
- Chakhmouradian, A.R., Mitchell, R.H., Pankov, A.V., Chukanov, N.V. (1999): Loparite and 'metaloparite' from the Burpala alkaline complex, Baikal Alkaline Province (Russia). *Min. Mag.*, **63**, 519-534.
- Ercit, T.S., Hawthorne, F.C., Černý, P. (1994): The structural chemistry of kalipyrochlore, a "hydro-pyrochlore". *Can. Mineral.*, **32**, 415-20.
- Ganzev, A.A., Efimov, A.F., Lyubomilova, G.V. (1969): Plumbobetafite, a new mineral variety from the pyrochlore group. *Trudy Mineral. Muzeya AN SSSR*, **19**, 135-137 (in Russ.).
- Hogarth, D.D. (1989): Pyrochlore, apatite and amphibole: distinctive minerals in carbonatites. in "Carbonatites: Genesis and evolution" (K. Bell, ed). Unwyn Hyman, London, 105-48.
- Hogarth, D.D., Horne, J.E.T. (1989): Non-metamict uranoan pyrochlore and uranopyrochlore from tuff near Ndale, Fort Portal area, Uganda. *Min. Mag.*, **53**, 257-262.
- Horváth, L. & Gault, R.A. (1990): The mineralogy of Mont Saint-Hilaire, Québec. *Mineral. Rec.*, **21**, 285-359.
- Ifantopulo, T.N. & Osokin, E.D. (1979): Accessory loparite from a stratified alkaline intrusion. in "New data on the mineralogy of alkaline formations". IMGRE Press, Moscow, 20-28 (in Russ.).
- Johan, V. & Johan, Z. (1994): Accessory minerals of the Cínovec (Zinnwald) granite cupola, Czech Republic. Part 1: Nb-, Ta- and Ti-bearing oxides. *Mineral. Petrol.*, **51**, 323-343.
- Kapustin, Yu.L. (1989): Rare earth-bearing pyrochlore from agpaite pegmatites of the Khibina massif. *Trudy Mineral. Muzeya AN SSSR*, **36**, 155-161 (in Russ.).
- (1991): Pyrochlore-group minerals from the alkaline massifs of Tuva. *Izvestiya AN SSSR, Ser. Geol.*, **1991(3)**, 105-113 (in Russ.).
- Knudsen, C. (1989): Pyrochlore group minerals from the Qaqarssuk carbonatite complex. in "Lanthanides, tantalum and niobium", (P. Möller, P. Černý & F. Saupé, eds.). Springer-Verlag, Berlin, 80-99.
- Khomiyakov, A.P. (1995): "Mineralogy of hyperagpaite alkaline rocks". Oxford Scientific Publications, Clarendon Press, Oxford, 222 pp.
- Kogarko, L.N., Kononova, V.A., Orlova, M.P., Woolley, A.R. (1995): "Alkaline rocks and carbonatites of the world. Part 2: Former USSR". Chapman & Hall, London, U.K., 226 pp.
- Kogarko, L.N., Williams, C.T., Osokin, E.D. (1996): Evolution of the composition of loparite from the Lovozero massif. *Geokhim.*, **1996(4)**, 294-297.
- Korobeinikov, A.N. & Laajoki, K. (1994): Petrological aspects of the evolution of clinopyroxene composition in the intrusive rocks of the Lovozero alkaline massif. *Geochem. Int.*, **31**, 69-76.
- Kostyleva-Labuntsova, E.E., Borutskii, B.E., Sokolova, M.N., Shlyukova, Z.V., Dorfman, M.D., Dudkin, O.B., Kozyreva, L.V., Ikorskii, S.V. (1978): "The Mineralogy of the Khibina massif". Nauka press, Moscow (in Russ.), 586 pp. (in Russ.).
- Krivokoneva, G.K. & Sidorenko, G.A. (1971): The essence of the metamict transformation in pyrochlores. *Geochem. Int.*, **8(1-2)**, 113-122.
- Krivokoneva, G.K., Portnov, A.M., Semenov, E.I., Dubakina, L.S. (1979): Komarovite – silicified Pyrochlore. *Doklady AN SSSR, Earth Sci. Sect.*, **248**, 127-130.
- Krivovichev, S.V., Chakhmouradian, A.R., Mitchell, R.H., Chukanov, N.V., Filatov, S.K. (2000): Crystal structure of isolushite, (Na,La)(Nb,Ti)O<sub>3</sub>, and its synthetic analogue. *Eur. J. Mineral.*, **12**, 597-607.
- Lumpkin, G.R. & Ewing, R.C. (1995): Geochemical alteration of pyrochlore group minerals: Pyrochlore subgroup. *Am. Mineral.*, **80**, 732-743.

- Mariano, A.N., Lumpkin, G.R., Leung, S.H.F. (1997): Ideal and defect pyrochlores from the Araxá carbonatite complex and laterite, Alto Paranaíba Province, Brazil. *Ottawa '97 GAC/MAC Annual Meeting, Abstr. Vol.*, A-97.
- Marochkina, M.N. (1990): Pyrochlore from aegirine-feldspar veins of the Khibina massif. in "New data on the mineralogy of Karelo-Kola region". Petrozavodsk, Russia, 5-24 (in Russ.).
- Mitchell, R.H. (1996): Perovskites: A revised classification scheme for an important rare earth element host in alkaline rocks. in "Rare earth minerals: Chemistry, origin and ore deposits" (A.P. Jones, F. Wall and C.T. Williams, eds.). Chapman and Hall, London, 41-76.
- Mitchell, R.H. & Chakhmouradian, A.R. (1996): Compositional variation of loparite from the Lovozero alkaline complex, Russia. *Can. Mineral.*, **34**, 977-990.
- , — (1999): Solid solubility in the system NaLREETi<sub>2</sub>O<sub>6</sub> - ThTi<sub>2</sub>O<sub>6</sub> (LREE, light rare-earth elements): Experimental and analytical data. *Phys. Chem. Minerals*, **26**, 396-405.
- Mitchell, R.H., Burns, P.C., Chakhmouradian, A.R. (2000): The crystal structures of loparite-(Ce). *Can. Mineral.*, **38**, 145-152.
- Ohnenstetter, D. & Piantone, P. (1992): Pyrochlore-group minerals in the Beauvoir peraluminous leucogranite, Massif Central, France. *Can. Mineral.*, **30**, 771-784.
- Pekov, I.V. (2000): "Lovozero massif: History, pegmatites, minerals". Ocean Pictures, Moscow. 480 p.
- Reguir, E.P., Chakhmouradian, A.R., Evdokimov, M.D. (1999): The mineralogy of a unique baratovite- and miserite-bearing quartz-albite-aegirine rock from the Dara-i-Pioz complex, Northern Tadjikistan. *Can. Mineral.*, **37**, 1369-1384.
- Reid, A.F., Li, C., Ringwood, A.E. (1977): High-pressure silicate pyrochlores Sc<sub>2</sub>Si<sub>2</sub>O<sub>7</sub> and In<sub>2</sub>Si<sub>2</sub>O<sub>7</sub>. *J. Solid State Chem.*, **20**, 219-226.
- Semenov, E.I. (1972): "The mineralogy of the Lovozero alkaline massif". Nauka Press, Moscow, 308 p. (in Russ.).
- Semenov, E.I., Sørensen, H., Katajeva, Z.T. (1968): On the mineralogy of pyrochlore from the Ilímaussaq alkaline intrusion, South Greenland. *Medd. Grønland*, **181** (7), 9-24.
- Semenov, E.I., Spitsyn, A.N., Burova, Z.N. (1963): Hydropyrochlore from the Lovozero alkaline massif. *Doklady AN SSSR*, **150**, 1128-1130 (in Russ.).
- Skorobogatova, N.V., Sidorenko, G.A., Dorofeeva, K.A., Stolyarova, T.I. (1966): On plumbopyrochlore. *Trudy IMGRE*, **30**, 84-95 (in Russ.).
- Uher, P., Černý, P., Chapman, R., Határ, J., Miko, O. (1998): Evolution of Nb,Ta-oxide minerals in the Prašivá granitic pegmatites, Slovakia. II. External hydrothermal Pb,Sb overprint. *Can. Mineral.*, **36**, 535-545.
- Vlasov, K.A., Kuz'menko, M.V., Es'kova, E.M. (1966): "The Lovozero alkali massif". Oliver & Boyd, Edinburgh, 627 p.
- Voloshin, A.V. & Polezhaeva, L.I. (1979): A study of composition of strontian hydropyrochlore. *Konst. Svoistva Mineral.*, **13**, 18-25 (in Russ.).
- Voloshin, A.V., Bukanov, V.V., Polezhaeva, L.I. (1981): Plumbomicrolite and plumbopyrochlore from amazonite pegmatites of the Kola Peninsula. *Mineral. Zhurnal (Kiev)*, **3**(5), 20-34 (in Russ.).
- Voloshin, A.V., Pakhomovskiy, Ya.A., Pushcharovskiy, D.Yu., Nadezhina, T.N., Bakhchisaraitsev, A.Yu., Kobylashev, Yu.S. (1989): Strontio-pyrochlore: composition and structure. *Trudy Mineral. Muzeya AN SSSR*, **36**, 12-24 (in Russ.).
- Voloshin, A.V., Pakhomovskiy, Ya.A., Bakhchisaraitsev, A.Yu. (1993): Plumbobetafite from amazonite and pegmatites of the Western Keivy (Kola Peninsula). *Mineral. Zhurnal (Kiev)*, **15**, 76-80 (in Russ.).
- Wallace, G.M., Whalen, J.B., Martin, R.F. (1990): Agpaitic and miaskitic nepheline syenites of the McGerrigle plutonic complex, Gaspé, Québec: An unusual petrological association. *Can. Mineral.*, **28**, 251-266.
- Williams, C.T. (1996): The occurrence of niobian zirconolite, pyrochlore and baddeleyite in the Kovdor carbonatite complex, Kola Peninsula, Russia. *Min. Mag.*, **60**, 639-646.
- Zadov, A.E., Chukanov, N.V., Pekov, I.V. (1999): Uranopyrochlore from an ultra-alkaline pegmatite in the Lovozero complex. in "Carbonatites of the Kola Peninsula" (A.G. Bulakh *et al.*, eds). St. Petersburg State University Press, St. Petersburg, 57-58 (in Russ.).

Received 3 May 2001

Modified version received 4 January 2002

Accepted 4 February 2002